Virology 443 (2013) 20–27

Contents lists available at SciVerse ScienceDirect

Virology

journal homepage: www.elsevier.com/locate/yviro

The ATPase of the phi29 DNA packaging motor is a member of the hexameric AAA+ superfamily ☆

Chad Schwartz [1], Gian Marco De Donatis [1], Huaming Fang [1], Peixuan Guo *

Nanobiotechnology Center, College of Pharmacy and Markey Cancer Center, University of Kentucky, Lexington, KY, USA

ARTICLE INFO

Available online 22 May 2013

Keywords:
Revolution Motor
Hexameric ATPase
Nanobiotechnology
Nanomotor
Push through a one-way valve

ABSTRACT

The AAA+ superfamily of proteins is a class of motor ATPases performing a wide range of functions that typically exist as hexamers. The ATPase of phi29 DNA packaging motor has long been a subject of debate in terms of stoichiometry and mechanism of action. Here, we confirmed the stoichiometry of phi29 motor ATPase to be a hexamer and provide data suggesting that the phi29 motor ATPase is a member of the classical hexameric AAA+ superfamily. Native PAGE, EMSA, capillary electrophoresis, ATP titration, and binomial distribution assay show that the ATPase is a hexamer. Mutations in the known Walker motifs of the ATPase validated our previous assumptions that the protein exists as another member of this AAA+ superfamily. Our data also supports the finding that the phi29 DNA packaging motor uses a revolution mechanism without rotation or coiling (Schwartz et al., this issue).

Introduction

The superfamily of AAA+ motors (ATPases associated with diverse cellular activities) plays a key role in several assorted functions, and many members of this clade of ATPases often fold into hexameric structures (Mueller-Cajar et al., 2011; Wang et al., 2011). Despite their diversity, the common characteristic of this family is their ability to convert chemical energy from the hydrolysis of the γ-phosphate bond of ATP into a protein conformational change. This change of conformation generates a loss of affinity for its substrate and exerts a mechanical movement, which in turn is used to either make or break contacts between macromolecules, resulting in local or global protein unfolding, assembly or disassembly of complexes, or transport of macromolecules relative to each other. These activities underlie processes critical to DNA repair, replication, recombination, chromosome segregation, dsDNA transportation, membrane sorting, cellular reorganization, and many other functions (Martin et al., 2005; Ammelburg et al., 2006).

DsDNA viruses package their DNA genome into a preformed protein shell called a procapsid, with the aid of a nanomotor (Feiss and Rao, 2012; Guo and Lee, 2007; Fang et al., 2012; Zhang et al., 2012). Since 1978, it has been popularly believed that viral DNA packaging motors run through a five-fold/six-fold mismatch rotation mechanism (Hendrix, 1978). An RNA component (pRNA) was discovered on the phi29 DNA packaging motor (Guo et al., 1987a), and subsequently, pRNA was determined to exist as a hexameric ring (Guo et al., 1998; Zhang et al., 1998). Based on this structure, it was proposed that the mechanism of the phi29 viral DNA packaging motor is similar to that used by other hexameric DNA tracking motors of the AAA+ family of proteins (Guo et al., 1998). A debate subsequently developed concerning whether the RNA and ATPase of the motor exist as hexamers (Zhang et al., submitted for publication, 2012, 1998; Guo et al., 1998; Shu et al., 2007; Xiao et al., 2008; Ibarra et al., 2000) or as pentamers (Moffitt et al., 2009; Yu et al., 2010; Chistol et al., 2012). The differing viewpoints have not yet been fully reconciled, but we have recently shown using X-ray diffraction, AFM imaging, and single molecule studies that the motor consists of three coaxial rings geared by hexameric pRNA (Zhang et al., submitted for publication) (Fig. 1). The force generation mechanism of the phi29 DNA packaging motor is still under debate (Moffitt et al., 2009; Aathavan et al., 2009; Jing et al., 2010; Zhang et al., 2012; Geng et al., 2011; Fang et al., 2012; Schwartz et al., 2012).

The phi29 DNA packaging motor reconstituted in the defined system more than twenty years ago (Guo et al., 1986) is one of the most well-studied biomotor systems and has also proven to be one of the most powerful molecular motors (Smith et al., 2001;

* Correspondence to: William Farish Endowed Chair in Nanobiotechnology, School of Pharmacy, University of Kentucky, 565 Biopharmaceutical Complex, 789 S. Limestone Street, Lexington, KY 40536, USA.
E-mail address: peixuan.guo@uky.edu (P. Guo).
[1] These authors contributed equally.

0042-6822/$ - see front matter © 2013 The Authors. Published by Elsevier Inc. All rights reserved.
http://dx.doi.org/10.1016/j.virol.2013.04.004

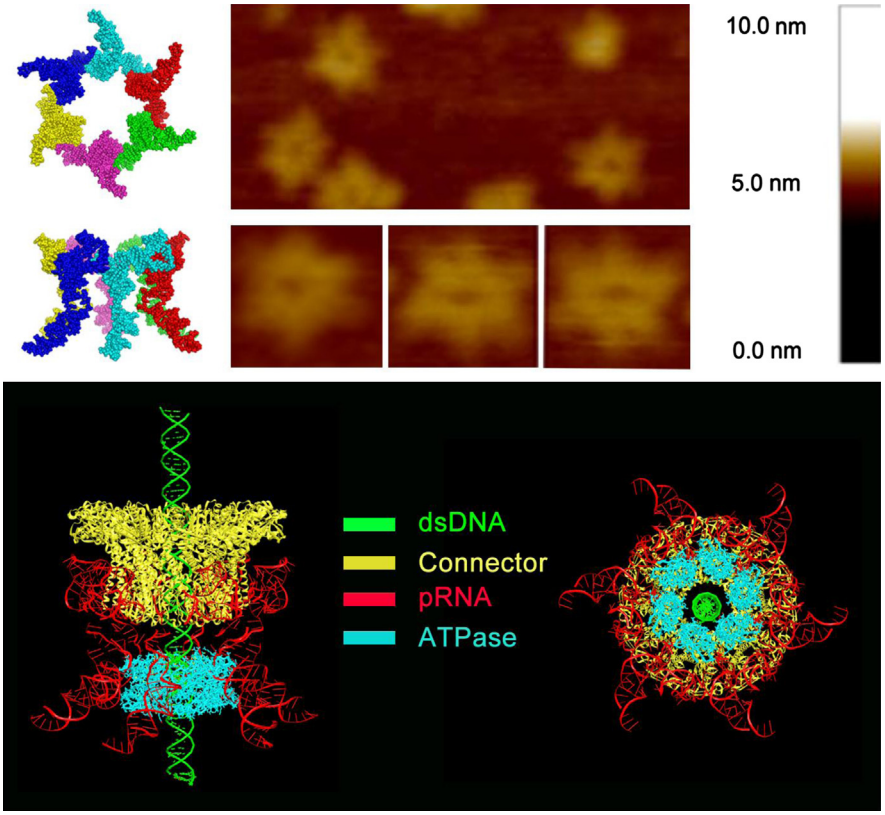

Fig. 1. Depiction of the phi29 DNA packaging motor structure and function. A schematic of hexameric pRNA (left, top) and AFM images of loop-extended hexameric pRNA (top, right) (Shu et al., in press). Illustrations of the phi29 DNA packaging motor and a pRNA hexamer: side view (bottom, left) and bottom view (bottom, right).

Rickgauer et al., 2008), capable of generating forces up to 57–110 pN. The viral DNA packaging mechanism has been studied extensively (Simpson et al., 2000; Aathavan et al., 2009; Smith et al., 2001; Earnshaw and Casjens, 1980; Hendrix, 1998; Johnson et al., 2007; Rao and Black, 1985; Guo et al., 1998; Sun et al., 2007; Zhang et al., 1998; Zheng et al., 2008; Agirrezabala et al., 2005; Butcher et al., 1995; Dubé et al., 1993; Gutierrez et al., 1994; Lebedev et al., 2007; Orlova et al., 2003; Shu et al., 2007; Sousa and Padilla, 1995; Stewart et al., 1993; Xiang et al., 2006; Hugel et al., 2007). The phi29 DNA packaging motor is composed of a dodecameric connector at the vertex of the procapsid, geared by a pRNA ring (Guo et al., 1987a) which encircles the N-terminus of the connector (Xiao et al., 2005, 2008; Atz et al., 2007), and a ring of gp16 which functions as an ATPase to drive the motor (Guo et al., 1987c; Ibarra et al., 2001). The connector was recently revealed to only allow for unidirectional movement of dsDNA (Jing et al., 2010), and a model using a "push through a one-way valve" mechanism was described (Schwartz et al., 2012; Fang et al., 2012) which agrees nicely with the previously proposed ratchet (Serwer, 2003) and compression (Ray et al., 2010a, 2010b) models. This mechanism describes dsDNA as being pushed through the connector channel by the ATPase gp16 while the connector functions like a valve to prevent DNA from slipping out of the capsid during the packaging process. This entropically unfavorable process is accomplished using ATP as an energy source (Black, 1989; Feiss and Rao, 2012; Casjens, 2011; Guo and Lee, 2007).

The ATPase gp16 is the most critical part of the phi29 DNA packaging motor. It provides energy for the motor by hydrolyzing ATP, converting energy obtained from breaking a chemical bond into physical motion. This enzyme possesses the typical Walker A and Walker B motifs (Guo et al., 1987c) as found in many other well-characterized AAA+ proteins (Burroughs et al., 2007; Iyer et al., 2004). The protein has been shown to bind to the 5′/3′ paired helical region of pRNA (Lee and Guo, 2006; Koti et al., 2008), and furthermore, its ATPase activity could be stimulated by both pRNA and DNA (Guo et al., 1987c; Lee et al., 2008; Ibarra et al., 2001; Grimes and Anderson, 1990). Intermediates in DNA packaging have been isolated (Guo et al., 1987b; Smith et al., 2001; Koti et al., 2008; Shu and Guo, 2003), and models of gp16 supercoiling dsDNA have been proposed (Grimes and Anderson, 1997; Koti et al., 2008).

Here, the oligomeric state of the ATPase has been extensively investigated in order to better understand the DNA translocation mechanism. We conclusively determined that the motor ATPase forms a hexamer in a concentration dependent manner and upon binding to its substrate dsDNA. Furthermore, the major motifs of the ATPase have now been identified and we have shown through mutation analysis that the phi29 ATPase is a member of the hexameric AAA+ superfamily.

Results

Phi29 DNA packaging motor contains three coaxial rings

The phi29 DNA packaging motor consists of three major structural components: the connector, pRNA, and ATPase gp16 (Fig. 1). Extensive studies (Guo, 2002; Green et al., 2010; Ibarra et al., 2000; Xiao et al., 2008; Zhang et al., 1998; Shu et al., 2007; Trottier and Guo, 1997; Chen et al., 1997) of the pRNA and a recent crystal structure (Zhang et al., 2013) has revealed that pRNA exists as a hexamer, as also confirmed by AFM (Shu et al., in press). These data show that the three coaxial rings are connected to each other with fixed stoichiometry.

Native PAGE, EMSA, and CE reveal hexameric ATPase

Fusion of eGFP to the N-terminus of gp16 results in fluorescent gp16 (eGFP-gp16) that shows similar biological activity as native gp16 (Lee et al., 2009). eGFP-gp16 yields six distinct fluorescent bands on a native PAGE gel which separates solely on the basis of mass (see Materials and methods), indicative of six monomers oligomerizing to form a hexamer (Fig. 2A). The monomer and all even numbered oligomer bands have a higher intensity than the trimer and pentamer, suggesting that the assembly sequence is monomer to dimer, to tetramer and finally to hexamer, such that the final gp16 oligomeric state is likely a trimer of dimers, as in other ATPases (Sim et al., 2008; Skordalakes and Berger, 2006; Ziegelin et al., 2003; Sim et al., 2008). In addition, as the concentration of gp16 is increased, the intensity of the hexamer band increased significantly, while the intensity of smaller oligomers remains fairly constant, further suggesting that a hexamer is the final oligomeric state. Finally, the presence of eGFP-gp16 hexamer was further confirmed by stoichiometric ratio assays as discussed in the following sections.

Electrophoretic mobility shift assays (EMSA) were employed with the fluorescent eGFP-gp16 and with a short 40 bp dsDNA fragment conjugated to a cy3 fluorophore. The two components were mixed together with ATP and a non-hydrolyzable ATP analog (γ-S-ATP) (Fig. 2B). The ATPase bound more tightly to the dsDNA upon addition of γ-S-ATP (Fig. 2B, lane 6) as observed previously (Schwartz et al., 2012). Furthermore, after addition of ATP to the gp16:DNA complex, two distinct ATPase bands were present (Fig. 2B, lanes 7,8), perhaps representative of two different conformational states of gp16.

We repeated the EMSA with increasing amounts of ATPase and a fixed amount of dsDNA to determine the stoichiometry of the ATPase bound to dsDNA. As the molar concentration ratio of gp16: dsDNA reached 6:1, free dsDNA (bottom band, Fig. 3A Cy3 channel) shifted nearly entirely to the bound state (top yellow band, lane 6). Capillary electrophoresis was used to validate the qualitative EMSA data. In this case, the amount of gp16 was held at 3 μM, mainly due to the stickiness of the protein in the small capillary, and the [dsDNA] was varied in the reaction mixture. The fluorescent peak corresponding to the DNA:protein complex was quantified over a range of dsDNA concentrations. A plateau was achieved at 0.5 μM DNA bound, representing a ratio of DNA: protein of 1:6, further arguing that the gp16 ATPase is a hexamer (Fig. 3B).

Mutations of known motifs suggest that phi29 gp16 is a member of the AAA+ superfamily of ATPases

Gp16 contains well-conserved motifs responsible for ATP binding (Walker A and Arginine finger) and ATP hydrolysis (Walker B), typical of all AAA+ proteins. The Walker A motif was previously identified, but the Walker B motif had not been determined (Guo et al., 1987c). Sequence alignment with AAA+

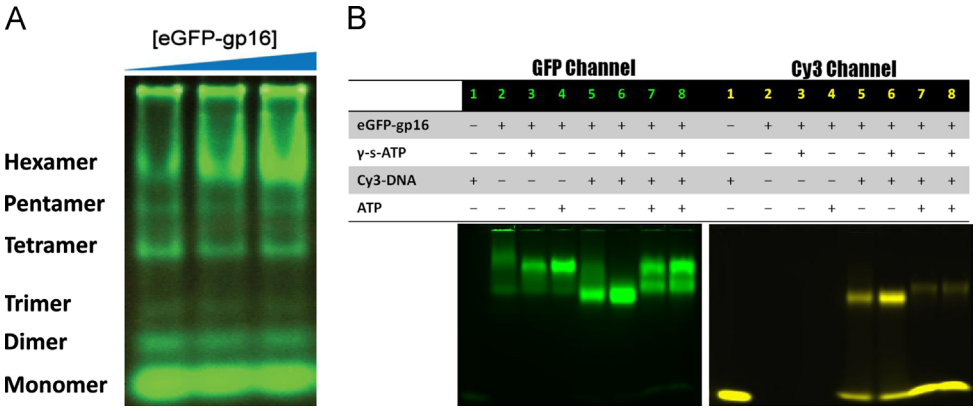

Fig. 2. (**A**) 6% Native PAGE using a non-denaturing detergent which fractionates by size reveals distinct bands characteristic of six oligomeric states; the top, hexameric band increased as the concentration of protein is increased (15 μM, 17.5 μM, 20 μM). Oligomeric states were assigned based on the mobility of marker proteins in the Native PAGE Mark kit. (**B**) EMSA of native eGFP-gp16 (3 μM) with short, 40 bp Cy3-dsDNA (300 nM) and ATP (30 mM) or γ-S-ATP (1.25 mM). The GFP channel (left) shows migration of the ATPase, whereas the Cy3 channel (right) indicates the migration of the dsDNA. Two distinct states of ATPase exist after addition of ATP to the gp16:DNA complex.

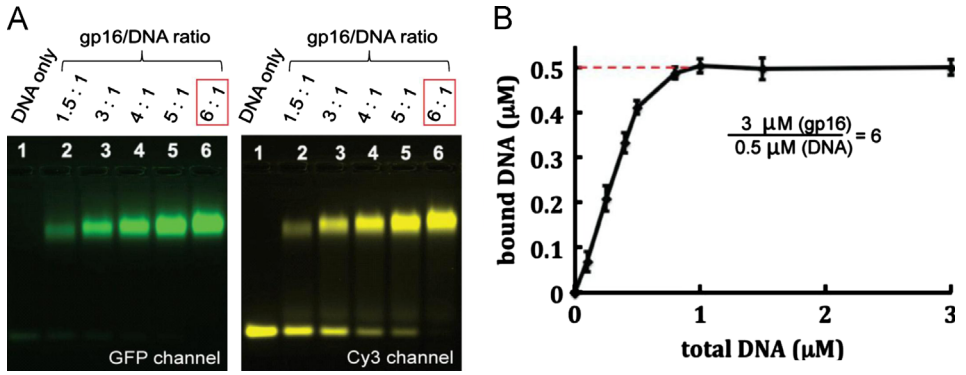

Fig. 3. ATPase gp16 binds to DNA in a 6:1 molar ratio. EMSA of 3 μM gp16 and dsDNA (**A**) where free dsDNA band disappears (bottom right) as the molar ratio of gp16: dsDNA reaches 6:1. (**B**) Capillary electrophoresis of eGFP-gp16 and Cy3-DNA complexes after quantification of fluorescent peaks. Data are plotted as a ratio of total DNA *versus* bound DNA and plateaus at 0.5 μM, a concentration six times less than the fixed molar concentration of ATPase gp16. (For interpretation of the references to color in this figure, the reader is referred to the web version of this article.)

proteins revealed the Walker B motif (hhhhDE) at residues 114–119 (TIVFDE), where 'h' represents hydrophobic residues.

To confirm the results of sequence alignment, relevant amino acids of both Walker A and Walker B motifs were mutated. For the Walker A motif, the previous mutant G27D was cloned. In the Walker B motif, two mutants were generated: E119A and D118E/E119D double mutant. The most important residues in Walker B are the aspartate (D) for its role in magnesium ion binding, and glutamate (E) responsible for the activation of a water molecule to perform a nucleophilic attack on the gamma phosphate of ATP. Both mutants were tested for their ability to hydrolyze ATP and to bind DNA.

Both mutants were subjected to the ATP hydrolysis assay (Lee et al., 2008). Only the wildtype ATPase hydrolyzed ATP (Fig. 4A); the Walker A G27D mutant is incapable of binding ATP while the Walker B mutant can bind, but cannot hydrolyze. We expanded our testing of the mutants in terms of DNA binding. Using the same capillary electrophoresis assay used for wildtype ATPase, we quantified the DNA bound peak of both mutants. In the presence of γ-S-ATP, the wildtype and Walker B mutant displayed similar DNA binding affinities. However, upon addition of ATP, the wildtype no longer remains bound to DNA as previously shown (Schwartz et al., 2012), but the Walker B D118E/E119D mutant retains its DNA binding capability, suggesting that this identified motif is in fact responsible for the catalytic step which pushes dsDNA away from gp16 upon hydrolysis.

Lastly, we attempted to validate our findings using EMSA (Fig. 4C). Gp16 ATPase and fluorescent DNA were mixed together and incubated at room temperature for 20 min. The samples were then loaded into an agarose gel. The top, green gel represents the fluorescent signal of the eGFP-conjugated ATPase; however, the bottom, yellow gel shows the migration of the cy3-fluorescent dsDNA. In the cy3 gel, the upper bands are representative of DNA bound to gp16 ATPase as the protein retards the migration of the short DNA. However, the bottom bands are free DNA as the negatively-charged strand of nucleotides quickly migrates to the positive electrode. Again, the wildtype gp16 ATPase exhibits high affinity to dsDNA with addition of γ-S-ATP (lane 3), but diminished affinity with ATP or no phosphate analog (lanes 2,4). The Walker A G27D mutant has diminished binding affinity in all cases (lanes

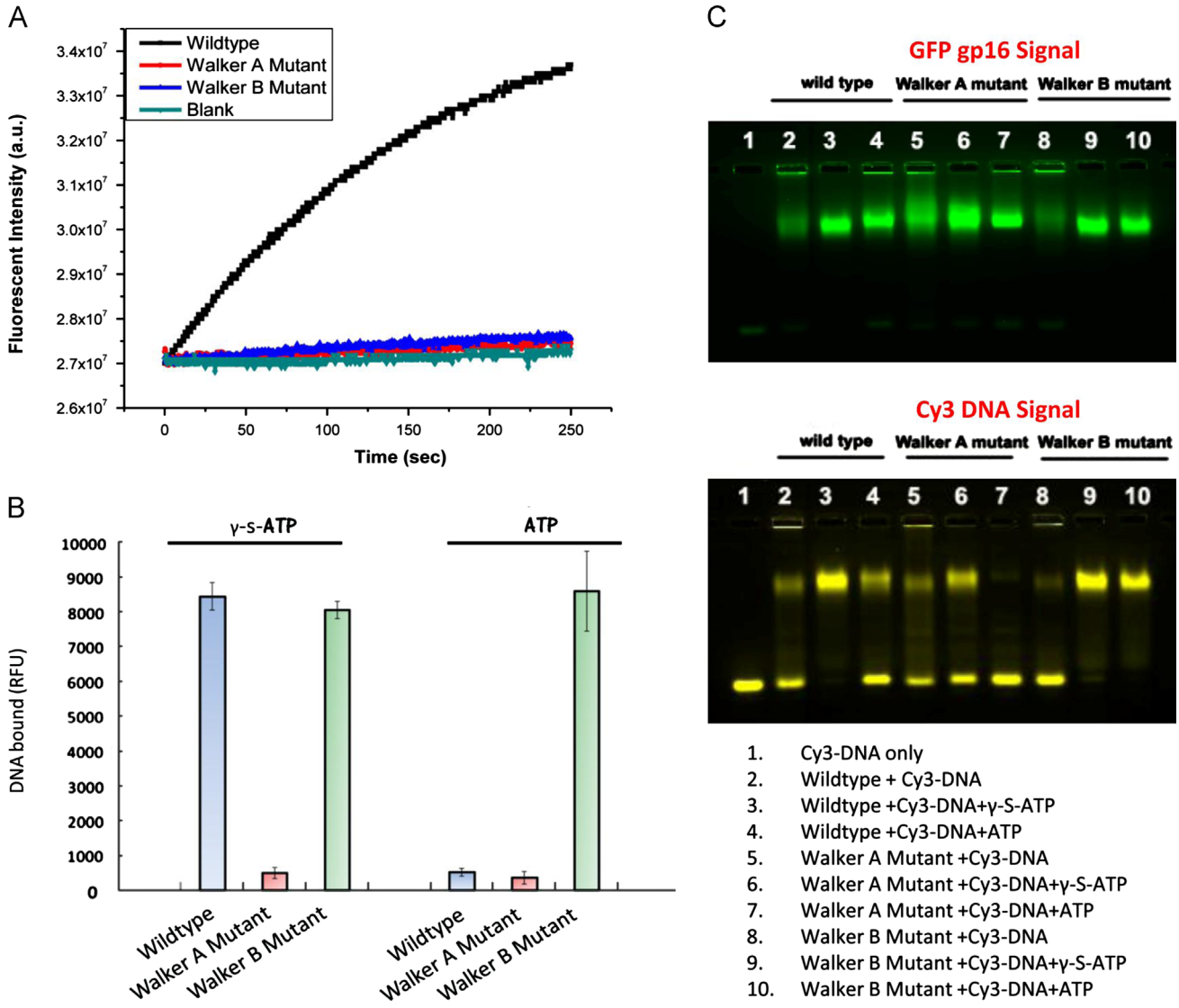

Fig. 4. ATPase gp16 contains a Walker A and Walker B motif typical of the AAA+ family. Assay of gp16 ATPase activity was described previously (Lee et al., 2008) (**A**). Walker A G27D and Walker B D118E/E119D mutants of gp16 prevent ATP hydrolysis. Capillary electrophoresis quantification of dsDNA binding to mutant and wildtype gp16 (**B**). Walker B D118E/E119D mutant retains binding capability to dsDNA despite addition of ATP. EMSA of mutant and wildtype ATPase (**C**). DNA binding is diminished with the Walker A G27D mutant but is retained in the Walker B D118E/E119D mutant with addition of ATP or γ-S-ATP. The results were comparable with Walker B E119A mutant. (For interpretation of the references to color in this figure, the reader is referred to the web version of this article.)

5–7), albeit higher affinity with addition of γ-S-ATP, as this mutant is incapable of binding ATP which stabilizes the interaction between gp16 and dsDNA. Finally, the Walker B D118E/E119D mutant which previously has been shown to be incapable of hydrolyzing ATP, was incapable of binding without ATP (lane 8), but exhibited high affinity with both ATP and γ-S-ATP (lanes 9,10). Both the capillary electrophoresis quantification and the EMSA confirmed our hypothesis that the recently discovered Walker B motif of phi29 ATPase is responsible for ATP hydrolysis.

Binomial inhibition assays with Walker B mutants validate hexameric ATPase

We further demonstrated that hexameric gp16 was active in phi29 DNA packaging using a Walker B mutant gp16 and a binomial distribution analysis (Trottier and Guo, 1997; Chen et al., 1997). The Walker B D118E/E119D mutant gp16 is completely inactive in DNA packaging. The mutant protein was mixed with wild-type in different ratios ranging from 10% to 90% at limiting quantities, and the activity of the complex was assayed using the *in vitro* viral assembly system (Fig. 5) (Lee and Guo, 1994). In this experiment, we assume that both the mutant and wildtype have an equal chance of incorporation within the final oligomer for packaging. The dominant inhibitory activity of the Walker B mutant allowed an independent means of determining the stoichiometry of the ATPase (Trottier and Guo, 1997).

In these trials, we assumed that the stoichiometry, Z, of the ATPase gp16 in the complex lies between 1 and 12. Different concentrations of wildtype gp16 were mixed with the inactive Walker B mutant and used for *in vitro* assembly reactions. We used a binomial distribution of $(p+q)^Z$, where p and q represent the ratio of wildtype and mutant subunits within the gp16 oligomer, respectively (Trottier and Guo, 1997). Following expansion of the binomial, we generated 12 theoretical curves corresponding to a stoichiometry of 1–12 using a plot of motor activity (in this case, production of phi29 virions) against the ratio of the Walker B mutant to wildtype. The empirical data almost perfectly overlap with the theoretical curve in slope and shape representative of a stoichiometry of 6, thereby confirming that the motor complex is hexameric (Fig. 5).

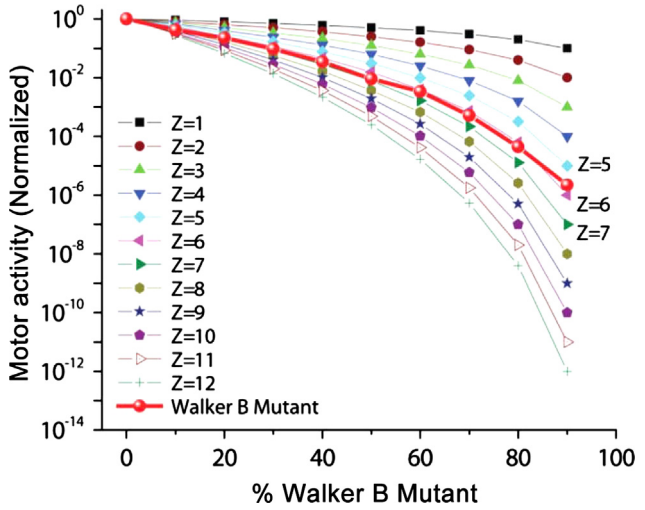

Fig. 5. Viral assembly inhibition assay using a binomial distribution revealing that gp16 is a hexamer in the DNA packaging motor (Trottier and Guo, 1997). Theoretical plot of percent Walker B mutant gp16 *versus* yield of infectious virions in *in vitro* phage assembly assays. Predictions were made with the equation $(p+q)^Z = \binom{Z}{0}p^Z + \binom{Z}{1}p^{Z-1}q + \binom{Z}{2}p^{Z-2}q^2 + \cdots + \binom{Z}{Z-1}pq^{Z-1} + \binom{Z}{Z}q^Z = \sum_{M=0}^{Z}\binom{Z}{M}p^{Z-M}q^M$, where p is the percentage of wild-type eGFP-gp16; q is the percentage of eGFP-gp16/ED; Z, is the total number of eGFP-gp16 per procapsid or gp3-DNA; M is the number of mutant eGFP-gp16 in the phi29 DNA packaging motor; and $p+q=1$ (Trottier and Guo, 1997).

Discussion

For many years, there has been a debate as to the stoichiometry of phi29 motor components. Many data has been shown by both camps as to the five-fold and six-fold nature of the gp16 ATPase and packaging RNA. However, both sides are in agreement that the stoichiometries of these two components exist in a 1:1 ratio. It has previously been shown that the symmetry remains uniform between the ATPase and pRNA whether it exists as a pentameric pRNA and pentameric ATPase or hexameric pRNA and hexameric ATPase, suggesting that the two work in unison, independent of the stoichiometry.

The data shown here indicate that gp16 ATPase is a member of the AAA+ superfamily of proteins, and similar to this family, the phi29 motor ATPase also exists in either a high or low affinity state for DNA substrate. Recently, it has been qualitatively demonstrated *via* EMSA (Schwartz et al., 2012) that the ATPase gp16 is capable of binding to dsDNA in the presence of γ-S-ATP. Fusion of a fluorescent tag on the ATPase did not affect its function or activity (Lee et al., 2009), but provided a marker for binding assays. In the previous reports, a small amount of Cy3-dsDNA was bound by eGFP-gp16 using the EMSA. However, stronger binding of gp16 to dsDNA was observed when gp16 was incubated with γ-S-ATP and dsDNA (Schwartz et al., 2012). Also in the previous reports, Förster Resonance Energy Transfer (FRET) analysis and sucrose sedimentation studies further validated our finding that the gp16/dsDNA complex is stabilized by addition of γ-S-ATP (Schwartz et al., 2012). Furthermore, the data confirmed that gp16 possesses both a DNA binding domain and a Walker A motif with which to bind ATP (Schwartz et al., 2012).

By sequence homology and point mutation analysis, both the Walker A and Walker B motifs have been shown to be involved in ATP hydrolysis in the ATPase of phi29 (Guo et. al., 1987a; Huang and Guo, 2003a). As expected, all the mutants were severely impaired in ATP hydrolysis activity and were similar to the Walker A mutant G27D, proving that the Walker A motif is responsible for binding of ATP. Regarding the ability to bind to DNA in the presence of γ-S-ATP, mutations in the walker A motif displayed a limited ability to bind DNA compared with the wild-type (Fig. 4B, C), most likely due to their impaired affinity for γ-S-ATP. On the contrary, the walker B mutants retained their binding affinity for DNA in the presence of γ-S-ATP and were also sufficient to bind DNA in the presence of ATP, confirming that the Walker B mutation only affects the ability to hydrolyze ATP but not the binding to the nucleotide.

Our data shows that in the absence of ATP, or its derivative γ-S-ATP, the binding of gp16 to DNA is reduced. However, after the addition of γ-S-ATP the binding efficiency of gp16 to DNA increased significantly (Fig. 4B, C). This suggests that ATP induces a change in gp16 that causes it to assume a high affinity conformation for dsDNA binding, a conclusion strengthened by the inability of the Walker A mutant protein, which cannot bind ATP, to elicit a conformational change. In the previous report, when ATP was added to the gp16-γ-S-ATP-dsDNA complex, rapid ATP hydrolysis was observed (Schwartz et al., 2012) and gp16 dissociated from the dsDNA. This indicates that after hydrolysis, gp16 undergoes a further conformational change that produces an external force against the dsDNA that pushes the substrate away from the motor complex by a power stroke. This phenomenon can

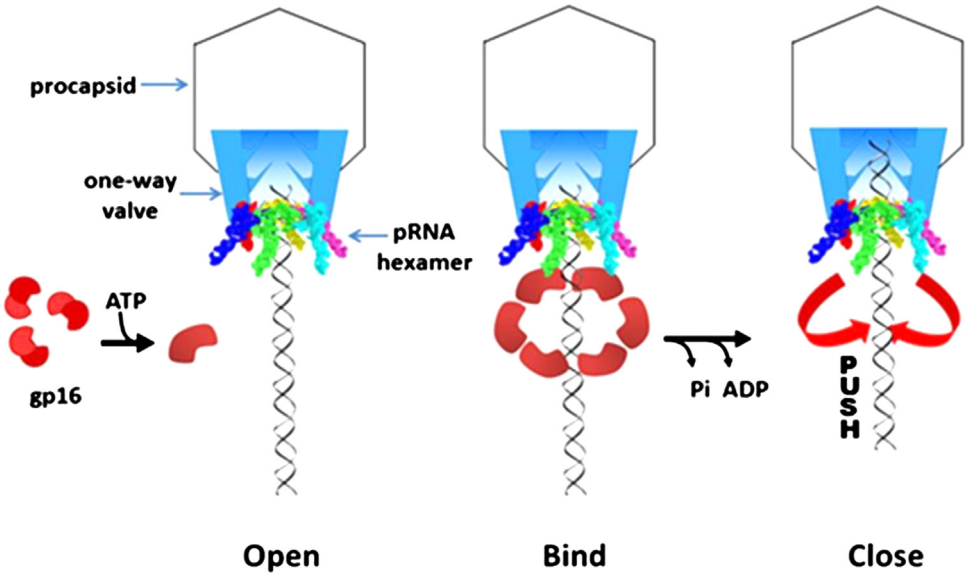

Fig. 6. Hexameric push through a one-way valve mechanism (Schwartz et al., 2012). A conformational change in the hexameric ATPase occurs subsequently after binding to ATP which confers an increase in binding affinity to dsDNA. Release of inorganic phosphate from the ATPase complex results in a power stroke to push the genomic dsDNA through the one-way valve of the connector portal protein into the capsid shell.

be seen in Fig. 2B in which the ATPase exists as two states after addition of ATP: DNA bound or expelled. However, introducing a mutation to the Walker B motif eliminated the catalytic force step. The data correlates nicely with other reports that Walker B mutants do not hydrolyze ATP, but bind strongly to DNA.

Gp16 is a DNA-dependent ATPase of the phi29 DNA packaging motor (Guo et al., 1987c; Huang and Guo, 2003a,b; Ibarra et al., 2001; Lee et al., 2008). Energy is provided to the motor through ATP. As aforementioned, non-hydrolyzable γ-S-ATP stalled and fastened the gp16/dsDNA complex. It has been found that the hydrolysis of ATP leads to the release of dsDNA from gp16. After ATP was added to the gp16/dsDNA/γ-S-ATP complex, the band representing the gp16/dsDNA complex disappeared (Schwartz et al., 2012). The release of dsDNA from the gp16/dsDNA/γ-S-ATP complex by ATP was also demonstrated by sucrose gradient sedimentation (Schwartz et al., 2012). Hydrolysis of ATP was confirmed when the purified gp16/dsDNA/γ-S-ATP hydrolyzed ATP after the addition of ATP to the purified complex (Schwartz et al., 2012). These results suggested that hydrolysis of ATP leads to the release of dsDNA from the gp16, forcing the DNA substrate away from the interior pocket of the ATPase, and lending to physical motion of genomic DNA towards the capsid.

Our data combining the stoichiometry of the ATPase and the sequential action previously elucidated (Schwartz et al., 2012), allows us to build upon our previous "push through a one-way valve" DNA packaging model. After binding to ATP, the ATPase undergoes a conformational change which significantly increases its affinity to dsDNA. An additional conformational change of the ATPase after release of inorganic phosphate causes gp16 to perform a power stroke to push dsDNA into the portal protein (Fig. 6).

The stoichiometry of the phi29 DNA packaging motor has long been a contentious subject. Here we have provided additional biochemical data showing that the ATPase gp16 consists of six subunits (Fig. 2A), upon binding to dsDNA (Fig. 3), and also in the active phi29 motor (Fig. 5). Furthermore, we have identified the classical Walker motifs typical of the hexameric AAA+ superfamily, and found that phi29 DNA packaging motor uses a revolution without rotation and coiling or generation of torque (Schwartz et al., this issue). In our accompanying paper in this issue, we show that the ATPase "hands off" the substrate dsDNA in a sequential action manner lending to revolution around the ATPase and connector protein. Our data leads to the conclusion that the hexameric stoichiometry and the mechanism of revolution for phi29 DNA packaging motor are in accordance with FtsK of the hexameric AAA+ superfamily, and we expect that most phages follow this "push through a one-way valve" *via* revolution mechanism (Zhao et al., in press; Schwartz et al., this issue).

Materials and methods

Cloning, mutagenesis and protein purification

The engineering of eGFP-gp16 and the purification of the gp16 fusion protein have been reported previously (Lee et al., 2009). The eGFP-gp16 mutants G27D, E119A, and D118E E119D were constructed by introducing mutations in the gp16 gene (Keyclone Technologies).

Measurement of gp16 ATPase activity

Enzymatic activity *via* fluorescent labeling was described previously (Lee et al., 2008). Briefly, a phosphate binding protein conjugated to a fluorescent probe that senses the binding of phosphate was used to assay ATP hydrolysis.

In vitro virion assembly assay

Purified *in vitro* components were mixed and were subjected to the virion assembly assay as previously described (Lee and Guo, 1994). Briefly, newly assembled infectious virions were inoculated with *Bacillus* bacteria and plated. Activity was expressed as the number of plaques formed per volume of sample (pfu/mL).

Statistical analysis and data plotting

Most statistical analysis was performed using Sigmaplot 11. The Hill coefficient was determined by nonlinear regression fitting of the experimental data to the following equation: $E=E_{max}\times(x)^n/(k_{app}+(x)^n)$, where E and E_{max} refer to the concentration of the

gp16/DNA complex, X is the concentration of ATP or ADP, K_{app} is the apparent binding constant, and n is the Hill coefficient.

CE experiments to determine ratio of gp16 to bound dsDNA

CE (capillary electrophoresis) experiments were performed on a Beckman MDQ system equipped with double fluorescence detectors (at 488 nm and 635 nm excitation wavelength). A bare borosilicate capillary with a total length of 60 cm and a 50 μm inner diameter was used. Assay conditions contained separation buffer of 50 mM Tris–HCl, 100 mM sodium borate at pH 8.00, 5 mM $MgCl_2$, 10% PEG 8000 (w/v), 0.5% acetone (v/v), 3 μM eGFP-gp16 monomer, and variable amounts of ATP/ADP and DNA.

Native PAGE of eGFP-gp16

Increasing amounts of eGFP-gp16 were loaded onto a 6% tris–glycine polyacrylamide gel in conjunction with the Native PAGE Mark kit (Invitrogen). This commercially available Native PAGE Mark kit uses a non-denaturing detergent to mildly solubilize and coats the protein with a negative charge. Thus, gel electrophoresis separates solely on the basis of mass. The gel was imaged using a Typhoon gel image scanner at an excitation wavelength of 488 nm.

Atomic force microscopy (AFM) imaging

APS mica was obtained by incubation of freshly cleaved mica in 167 nM 1-(3-aminopropyl) silatrane as described (Shlyakhtenko et al., 2003; Lyubchenko and Shlyakhtenko, 2009). Native PAGE purified RNA samples were diluted with 1xTMS buffer to a final concentration of 3–5 nM. Then, 5–10 μL of pRNA was immediately deposited on the APS mica surface. After 2 min incubation, excess samples were washed with DEPC treated water and dried under a flow of Argon gas. AFM images in air were acquired using MultiMode AFM NanoScope IV system (Veeco/Digital Instruments, Santa Barbara, CA) operating in tapping mode. Two types of AFM probes were used under tapping mode imaging in air: (1) regular tapping Mode Silicon Probes (Olympus from Asylum Research, Santa_Barbara, CA) with a spring constant of ~42 N/m and a resonant frequency between 300 kHz and 320 kHz. (2) non-contact NSG01_DLC probes (K-Tek Nanotechnology, Wilsonville, OR) with a spring constant of about 5.5 N/m and a resonance frequency between 120 kHz and 150 kHz.

Electrophoretic mobility shift assay (EMSA)

The fluorescently tagged protein that facilitates detection and purification was shown to possess similar assembly and packaging activity as compared to wildtype (Lee et al., 2009; Schwartz et al., 2012). Cy3-dsDNA (40 bp) was prepared by annealing two complementary DNA oligos containing a Cy3 label (IDT) at its 5′ ends and purified by a 10% polyacrylamide gel. Samples were prepared in 20 μl buffer A (20 mM Tris–HCl, 50 mM NaCl, 1.5% glycerol, 0.1 mM Mg^{2+}). Specifically, 1.78 μM eGFP-gp16 was mixed with 7.5 ng/μl of 40 bp Cy3-DNA in the presence or absence of ATP and γ-S-ATP. Samples were incubated at ambient temperature for 20 min and then loaded onto a 1% agarose gel (44.5 mM Tris, 44.5 mM boric acid) and electrophoresed at 4°C for 1 h at 8 V/cm. The eGFP-gp16 and Cy3-DNA samples were analyzed by a fluorescent LightTools Whole Body Imager using 488 nm and 540 nm excitation wavelengths for GFP and Cy3, respectively.

Acknowledgments

We would like to thank Dr. Guo-Min Li for his valuable comments; Yi Shu, Luda Shlyakhtenko, and Yuri Lyubchenko for the AFM images of pRNA hexamer; Zhengyi Zhao, Emil Khisamutdinov, and Hui Li for their diligent work on the animation figures; and Jeannie Haak for editing this manuscript. The work was supported by NIH Grants R01 EB012135, and U01 CA151648 to PG, who is a co-founder of Kylin Therapeutics, Inc., and Biomotor and Nucleic Acids Nanotech Development, Ltd.

References

Aathavan, K., Politzer, A.T., Kaplan, A., Moffitt, J.R., Chemla, Y.R., Grimes, S., Jardine, P.J., Anderson, D.L., Bustamante, C., 2009. Substrate interactions and promiscuity in a viral DNA packaging motor. Nature 461, 669–673.
Agirrezabala, X., Martin-Benito, J., Caston, J.R., Miranda, R., Valpuesta, J.M., Carrascosa, J.L., 2005. Maturation of phage T7 involves structural modification of both shell and inner core components. EMBO J. 24, 3820–3829.
Ammelburg, M., Frickey, T., Lupas, A.N., 2006. Classification of AAA+ proteins. J. Struct. Biol. 156, 2–11.
Atz, R., Ma, S., Gao, J., Anderson, D.L., Grimes, S., 2007. Alanine scanning and Fe-BABE probing of the bacteriophage phi29 prohead RNA-connector interaction. J. Mol. Biol. 369, 239–248.
Black, L.W., 1989. DNA Packaging in dsDNA bacteriophages. Annu.Rev. Microbiol. 43, 267–292.
Burroughs, A.M., Iyer, L.M., Aravind, L., 2007. Comparative genomics and evolutionary trajectories of viral ATP dependent DNA-packaging systems. In: Volff, J.-N. (Ed.), Gene and Protein Evlolution. Genome Dyn, pp. 48–65.
Butcher, S.J., Bamford, D.H., Fuller, S.D., 1995. DNA packaging orders the membrane of bacteriophage PRD1. EMBO J. 14, 6078–6086.
Casjens, S.R., 2011. The DNA-packaging nanomotor of tailed bacteriophages. Nat. Rev. Microbiol. 9, 647–657.
Chen, C., Trottier, M., Guo, P., 1997. New approaches to stoichiometry determination and mechanism investigation on RNA involved in intermediate reactions. Nucleic Acids Symp Ser 36, 190–193.
Chistol, G., Liu, S., Hetherington, C.L., Moffitt, J.R., Grimes, S., Jardine, P.J., Bustamante, C., 2012. High degree of coordination and division of labor among subunits in a homomeric ring ATPase. Cell 151, 1017–1028.
Dubé, P., Tavares, P., Lurz, R., van Heel, M., 1993. The portal protein of bacteriophage SPP1: a DNA pump with 13-fold symmetry. EMBO J. 12, 1303–1309.
Earnshaw, W.C., Casjens, S.R., 1980. DNA packaging by the double-stranded DNA bacteriophages. Cell 21, 319–331.
Fang, H., Jing, P., Haque, F., Guo, P., 2012. Role of channel lysines and "push through a one-way valve" mechanism of viral DNA packaging motor. Biophys. J. 102, 127–135.
Feiss, M., Rao, V.B., 2012. In: Rossmann, M.G., Rao, V.B. (Eds.), The bacteriophage DNA packaging machine viral molecular machines. Springer, US, pp. 489–509.
Geng, J., Fang, H., Haque, F., Zhang, L., Guo, P., 2011. Three reversible and controllable discrete steps of channel gating of a viral DNA packaging motor. Biomaterials 32, 8234–8242.
Green, D.J., Wang, J.C., Xiao, F., Cai, Y., Balhorn, R., Guo, P., Cheng, R.H., 2010. Self-assembly of heptameric nanoparticles derived from tag-functionalized phi29 connectors. ACS Nano 4, 7651–7659.
Grimes, S., Anderson, D., 1990. RNA dependence of the bateriophage phi29 DNA packaging ATPase. J. Mol. Biol. 215, 559–566.
Grimes, S., Anderson, D., 1997. The bacteriophage phi29 packaging proteins supercoil the DNA ends. J. Mol. Biol. 266, 901–914.
Guo, P., 2002. Structure and function of phi29 hexameric RNA that drive viral DNA packaging motor: review. Prog. Nucleic Acid Res. Mol. Biol. 72, 415–472.
Guo, P., Grimes, S., Anderson, D., 1986. A defined system for *in vitro* packaging of DNA-gp3 of the *Bacillus subtilis* bacteriophage phi29. Proc. Nat. Acad. Sci. USA 83, 3505–3509.
Guo, P., Erickson, S., Anderson, D., 1987a. A small viral RNA is required for *in vitro* packaging of bacteriophage phi29 DNA. Science 236, 690–694.
Guo, P., Peterson, C., Anderson, D., 1987b. Initiation events in *in vitro* packaging of bacteriophage ϕ29 DNA-gp3. J. Mol. Biol. 197, 219–228.
Guo, P., Peterson, C., Anderson, D., 1987c. Prohead and DNA-gp3-dependent ATPase activity of the DNA packaging protein gp16 of bacteriophage ϕ29. J. Mol. Biol. 197, 229–236.
Guo, P., Zhang, C., Chen, C., Trottier, M., Garver, K., 1998. Inter-RNA interaction of phage phi29 pRNA to form a hexameric complex for viral DNA transportation. Mol. Cell 2, 149–155.
Guo, P.X., Lee, T.J., 2007. Viral nanomotors for packaging of dsDNA and dsRNA. Mol. Microbiol. 64, 886–903.
Gutierrez, C., Freire, R., Salas, M., Hermoso, J.M., 1994. Assembly of phage phi29 genome with viral protein p6 into a compact complex. EMBO 13 (1), 269–276.
Hendrix, R.W., 1978. Symmetry mismatch and DNA packaging in large bacteriophages. Proc. Nat. Acad. Sci. USA 75, 4779–4783.
Hendrix, R.W., 1998. Bacteriophage DNA packaging: RNA gears in a DNA transport machine (minireview). Cell 94, 147–150.

Huang, L.P., Guo, P., 2003a. Use of acetone to attain highly active and soluble DNA packaging protein Gp16 of Phi29 for ATPase assay. Virology 312 (2), 449-457.
Huang, L.P., Guo, P., 2003b. Use of PEG to acquire highly soluble DNA-packaging enzyme gp16 of bacterial virus phi29 for stoichiometry quantification. J Virol Methods 109 (2), 235-244.
Hugel, T., Michaelis, J., Hetherington, C.L., Jardine, P.J., Grimes, S., Walter, J.M., Faik, W., Anderson, D.L., Bustamante, C., 2007. Experimental test of connector rotation during DNA packaging into bacteriophage phi29 capsids. Plos Biol. 5, 558–567.
Ibarra, B., Caston, J.R., Llorca, O., Valle, M., Valpuesta, J.M., Carrascosa, J.L., 2000. Topology of the components of the DNA packaging machinery in the phage phi29 prohead. J. Mol. Biol. 298, 807–815.
Ibarra, B., Valpuesta, J.M., Carrascosa, J.L., 2001. Purification and functional characterization of p16, the ATPase of the bacteriophage phi29 packaging machinary. Nucleic Acids Res. 29, 4264–4273.
Iyer, L.M., Makarova, K.S., Koonin, E.V., Aravind, L., 2004. Comparative genomics of the FtsK-HerA superfamily of pumping ATPases: implications for the origins of chromosome segregation, cell division and viral capsid packaging. Nucleic Acids Res. 32, 5260–5279.
Jing, P., Haque, F., Shu, D., Montemagno, C., Guo, P., 2010. One-way traffic of a viral motor channel for double-stranded DNA translocation. Nano Lett. 10 (9), 3620–3627.
Johnson, D.S., Bai, L., Smith, B.Y., Patel, S.S., Wang, M.D., 2007. Single-molecule studies reveal dynamics of DNA unwinding by the ring-shaped T7 helicase. Cell 129, 1299–1309.
Koti, J.S., Morais, M.C., Rajagopal, R., Owen, B.A., McMurray, C.T., Anderson, D., 2008. DNA packaging motor assembly intermediate of bacteriophage phi29. J. Mol. Biol. 381, 1114–1132.
Lebedev, A.A., Krause, M.H., Isidro, A.L., Vagin, A.A., Orlova, E.V., Turner, J., Dodson, E.J., Tavares, P., Antson, A.A., 2007. Structural framework for DNA translocation via the viral portal protein. EMBO J. 26, 1984–1994.
Lee, C.S., Guo, P., 1994. A highly sensitive system for the *in vitro* assembly of bacteriophage phi29 of *Bacillus subtilis*. Virology 202, 1039–1042.
Lee, T.J., Guo, P., 2006. Interaction of gp16 with pRNA and DNA for genome packaging by the motor of bacterial virus phi29. J. Mol. Biol. 356, 589–599.
Lee, T.J., Zhang, H., Liang, D., Guo, P., 2008. Strand and nucleotide-dependent ATPase activity of gp16 of bacterial virus phi29 DNA packaging motor. Virology 380, 69–74.
Lee, T.J., Zhang, H., Chang, C.L., Savran, C., Guo, P., 2009. Engineering of the fluorescent-energy-conversion arm of phi29 DNA packaging motor for single-molecule studies. Small 5, 2453–2459.
Lyubchenko, Y.L., Shlyakhtenko, L.S., 2009. AFM for analysis of structure and dynamics of DNA and protein–DNA complexes. Methods 47, 206–213.
Martin, A., Baker, T.A., Sauer, R.T., 2005. Rebuilt AAA+ motors reveal operating principles for ATP-fuelled machines. Nature 437, 1115–1120.
Moffitt, J.R., Chemla, Y.R., Aathavan, K., Grimes, S., Jardine, P.J., Anderson, D.L., Bustamante, C., 2009. Intersubunit coordination in a homomeric ring ATPase. Nature 457, 446–450.
Mueller-Cajar, O., Stotz, M., Wendler, P., Hartl, F.U., Bracher, A., Hayer-Hartl, M., 2011. Structure and function of the AAA+ protein CbbX, a red-type Rubisco activase. Nature 479, 194–199.
Orlova, E.V., Gowen, B., Droge, A., Stiege, A., Weise, F., Lurz, R., van, H.M., Tavares, P., 2003. Structure of a viral DNA gatekeeper at 10 A resolution by cryo-electron microscopy. EMBO J. 22, 1255–1262.
Rao, V.B., Black, L.W., 1985. Evidence that a phage T4 DNA packaging enzyme is a processed form of the major capsid gene product. Cell 42, 967–977.
Ray, K., Ma, J., Oram, M., Lakowicz, J.R., Black, L.W., 2010a. Single-molecule and FRET fluorescence correlation spectroscopy analyses of phage DNA packaging: colocalization of packaged phage T4 DNA ends within the capsid. J. Mol. Biol. 395, 1102–1113.
Ray, K., Sabanayagam, C.R., Lakowicz, J.R., Black, L.W., 2010b. DNA crunching by a viral packaging motor: compression of a procapsid-portal stalled Y-DNA substrate. Virology 398, 224–232.
Rickgauer, J.P., Fuller, D.N., Grimes, S., Jardine, P.J., Anderson, D.L., Smith, D.E., 2008. Portal motor velocity and internal force resisting viral DNA packaging in bacteriophage phi 29. Biophys. J. 94, 159–167.
Schwartz, C., Fang, H., Huang, L., Guo, P., 2012. Sequential action of ATPase, ATP, ADP, Pi and dsDNA in procapsid-free system to enlighten mechanism in viral dsDNA packaging. Nucleic Acids Res. 40, 2577–2586.
Schwartz, C., Zhang, H., Fang, H., De Donatis, G.M., Guo, P., 2013. Revolution rather than rotation of AAA+ hexameric phi29 nanomotor for viral dsDNA packaging without coiling. Virology, this issue, http://dx.doi.org/10.1016/j.virol.2013.04.019.
Serwer, P., 2003. Models of bacteriophage DNA packaging motors. J. Struct. Biol. 141, 179–188.
Shlyakhtenko, L.S., Gall, A.A., Filonov, A., Cerovac, Z., Lushnikov, A., Lyubchenko, Y.L., 2003. Silatrane-based surface chemistry for immobilization of DNA, protein–DNA complexes and other biological materials. Ultramicroscopy 97, 279–287.
Shu, D., Guo, P., 2003. Only one pRNA hexamer but multiple copies of the DNA-packaging protein gp16 are needed for the motor to package bacterial virus phi29 genomic DNA. Virology 309 (1), 108–113.
Shu, D., Zhang, H., Jin, J., Guo, P., 2007. Counting of six pRNAs of phi29 DNA-packaging motor with customized single molecule dual-view system. EMBO J. 26, 527–537.
Shu, Y., Haque, F., Shu,D., Li, W., Zhu, Z., Kotb, M., Lyubchenko, Y., Guo, P., Fabrication of 14 different RNA nanoparticles for specific tumor targeting without accumulation innormalorgans. RNA, in press. http://dx.doi.org/10.1261/rna.037002.112.
Sim, J., Ozgur, S., Lin, B.Y., Yu, J.H., Broker, T.R., Chow, L.T., Griffith, J., 2008. Remodeling of the human papillomavirus type 11 replication origin into discrete nucleoprotein particles and looped structures by the E2 protein. J. Mol. Biol. 375, 1165–1177.
Simpson, A.A., Tao, Y., Leiman, P.G., Badasso, M.O., He, Y., Jardine, P.J., Olson, N.H., Morais, M.C., Grimes, S., Anderson, D.L., Baker, T.S., Rossmann, M.G., 2000. Structure of the bacteriophage phi29 DNA packaging motor. Nature 408, 745–750.
Skordalakes, E., Berger, J.M., 2006. Structural insights into RNA-dependent ring closure and ATPase activation by the Rho termination factor. Cell 127, 553–564.
Smith, D.E., Tans, S.J., Smith, S.B., Grimes, S., Anderson, D.L., Bustamante, C., 2001. The bacteriophage phi29 portal motor can package DNA against a large internal force. Nature 413, 748–752.
Sousa, R., Padilla, R., 1995. A mutant T7 RNA polymerase as a DNA polymerase. EMBO J. 14, 4609–4621.
Stewart, P.L., Fuller, S.D., Burnett, R.M., 1993. Difference imaging of adenovirus: bridging the resolution gap between X- ray crystallography and electron microscopy. EMBO J. 12, 2589–2599.
Sun, S.Y., Kondabagil, K., Gentz, P.M., Rossmann, M.G., Rao, V.B., 2007. The structure of the ATPase that powers DNA packaging into bacteriophage t4 procapsids. Mol. Cell 25, 943–949.
Trottier, M., Guo, P., 1997. Approaches to determine stoichiometry of viral assembly components. J. Virol. 71, 487–494.
Wang, F., Mei, Z., Qi, Y., Yan, C., Hu, Q., Wang, J., Shi, Y., 2011. Structure and mechanism of the hexameric MecA–ClpC molecular machine. Nature 471, 331–335.
Xiang, Y., Morais, M.C., Battisti, A.J., Grimes, S., Jardine, P.J., Anderson, D.L., Rossmann, M.G., 2006. Structural changes of bacteriophage phi29 upon DNA packaging and release. EMBO J. 25, 5229–5239.
Xiao, F., Moll, D., Guo, S., Guo, P., 2005. Binding of pRNA to the N-terminal 14 amino acids of connector protein of bacterial phage phi29. Nucleic Acids Res. 33, 2640–2649.
Xiao, F., Zhang, H., Guo, P., 2008. Novel mechanism of hexamer ring assembly in protein/RNA interactions revealed by single molecule imaging. Nucleic Acids Res. 36, 6620–6632.
Yu, J., Moffitt, J., Hetherington, C.L., Bustamante, C., Oster, G., 2010. Mechanochemistry of a viral DNA packaging motor. J. Mol. Biol. 400, 186–203.
Zhang, F., Lemieux, S., Wu, X., St.-Arnaud, S., McMurray, C.T., Major, F., Anderson, D., 1998. Function of hexameric RNA in packaging of bacteriophage phi29 DNA *in vitro*. Mol. Cell 2, 141–147.
Zhang, H., Schwartz, C., De Donatis, G.M., Guo, P., 2012. Hexameric viral DNA packaging motor using a "push through a one-way valve" mechanism. Adv. Virus Res. 83, 415–465.
Zhang, H., Endrizzi, J.A., Shu, Y., Haque, F., Guo, P., Chi, Y.I., submitted for publication. Crystal structure of 3WJ core revealing divalent ion-promoted thermostability and assembly of the phi29 hexameric motor pRNA. RNA.
Zhao, Z., Khisamutdinov, E., Schwartz, C., Guo, P., Mechanism of one-way traffic of the hexameric DNA Translocation motor by means of anti-parallel helixes and four lysine layers. ACS Nano. 10.1021/nn4002775.
Zheng, H., Olia, A.S., Gonen, M., Andrews, S., Cingolani, G., Gonen, T., 2008. A conformational switch in bacteriophage P22 portal protein primes genome injection. Mol. Cell 29, 376–383.
Ziegelin, G., Niedenzu, T., Lurz, R., Saenger, W., Lanka, E., 2003. Hexameric RSF1010 helicase RepA: the structural and functional importance of single amino acid residues. Nucleic Acids Res. 31, 5917–5929.